THE INFLUENCE OF THE STRESS STATE ON FRACTURE TOUGHNESS — FURTHER RESULTS

D. AURICH, H. H. ERBE, R. HELMS, H. VEITH, J. ZIEBS
Bundesanstalt für Materialprüfung (BAM),
Unter den Eichen 87, D-1000 Berlin 45, Germany

Summary

Cracks in the pressure vessels are subjected to a biaxial nominal stress state. Conventional fracture mechanics disregard this situation and take into account the largest nominal stress only.

On the 4th SMiRT conference the practical importance of the influence of stress state on fracture has been already discussed and first experimental results have been presented. Now another type of specimen has been developed to realize a biaxial nominal stress state by biaxial plate bending. By variation of the support distance of bended plates the ratio of the nominal stresses can be changed within wide limits. The material ahead of a semi-elliptical surface crack in such a specimen is subjected to a local stress state of higher multi-axiality than under plane strain conditions.

The dimensions of the specimen were optimized by finite element method (FEM) for getting a homogeneous nominal stress state around the crack. This could be attained by an appropriate distribution of the loading points. Furthermore the stress distribution inside the plastic zone was analyzed. It was found that the second and third principal stress can be influenced considerably by nominal stress state. Therefore the plastic stress concentration factor $K_{\sigma p}$ varies in dependence on the nominal stress state. So a nominal stress acting parallel to the crack front additionally to the induced stress by constraint will enlarge $K_{\sigma p}$.

Tests were carried out in the temperature range of fracture at general yield T_{gy}. Results on biaxial bending were compared with those on usual three point bending. It is demonstrated that a biaxial nominal stress state shifts T_{gy} to higher temperature and reduces K_c or the nominal fracture stress in dependence on temperature.

1. Introduction

Cracks in pressure vessels are subjected to a biaxial nominal stress state. Conventional fracture mechanics however take into account only the largest nominal stress at plane strain conditions. To ventilate this discrepancy research has been already started as well on the influence of an additional stress acting in direction of crack extension [1, 2] as on the influence of an additional stress acting parallel to the crack front [3, 4]. Both situations are demonstrated in Fig. 1 on a penny shaped crack in a biaxial stressed structural member. Beside the crack opening force F_1 the force F_2 will induce as well an additional stress σ^e_{xx} in direction of crack extension at point Q as an additional stress σ^e_{zz} parallel to the crack front at point P. In continuing the work already referred at the 4th SMiRT conference [4] the influence of stress σ^e_{zz} on the fracture behaviour will be considered in this paper.

A nominal stress parallel to the crack front will not influence the stress intensity factor in the elastic range but will change the plastic zone size ahead the crack. This change can be verified by using the results e.g. of the Sneddon equations and fixing the elastic-plastic border by the criteria of the v. Mises hypothesis [3] . The result is that a tension stress will reduce the plastic zone size and a compression stress will increase it.

Nothing is known on the courses of the 2nd and 3rd principal stress within the plastic zone ahead a crack, but stresses and strains ahead 45^o-notches were calculated by finite element method for a linear hardening material [5]. From these results the Poisson's ratio as a function of x and so

$$\sigma^c_{zz} = \gamma\,(\sigma_{xx} + \sigma_{yy}) \qquad (1)$$

induced by constraint can be calculated. The stresses σ_{xx}, σ_{yy} and σ_{zz} normalized on the yield point σ_y in dependence on x are shown in Fig. 2 for a situation just post general yield where $F/F_{gy} = 1.065$ (F_{gy} = force at general yield). The results demonstrate that σ^c_{zz}/σ_y coincides with σ_{xx}/σ_y just at the point of the maximum of σ_{yy}/σ_y. For further increasing values of x σ^c_{zz}/σ_y even decreases below σ_{xx}/σ_y. This behaviour has been postulated already by Ewing and Griffith [6].

The materials response in dependence on stress state is given by a fracture hypothesis. For cleavage fracture the normal stress hypothesis in connection with the von Mises hypothesis is generally assumed to be relevant [7 - 9]. Hence the tendency to cleavage fracture is governed by the maximum plastic stress concentration factor

$$K_{\sigma p} = \frac{\sigma_{1max}}{\bar{\sigma}} = \frac{\sigma_{yymax}}{\sigma_y}, \qquad (2)$$

where σ_{1max} is the maximum of the 1st principal stress and $\bar{\sigma}$ the v. Mises equivalent stress. So tendency to cleavage fracture should increase by rising of $K_{\sigma p}$. This can be achieved by decrease of the equivalent stress $\bar{\sigma}$ which has a minimum if the 2nd principal stress is just the mean of the two other principal stresses. So for the special case of general yield from the results in Fig. 2 it can be deduced that the worst situation would be achieved in rising σ_{zz}/σ_y by an external nominal stress σ^e_{zz} parallel to crack front so that

$$\sigma_{zz} = \sigma^c_{zz} + \sigma^e_{zz} \qquad (3)$$

is the mean of $(\sigma_{xx} + \sigma_{yy})$. Whether the maximum of σ_{yy} will be influenced by σ^e_{zz} or not is not known at present. The increase of $K_{\sigma p}$ will cause an increase of temperature for general yield fracture which is very important in the range where the yield strength depends only weakly on temperature.

2. Development of Specimen

Formerly used double-T-shaped specimens [4] demonstrated some disadvantages. So it was very difficult to get homogeneous loading of the specimen without bending and early plastification in the transition radii restricted the temperatur range where the specimen could be used. The newly developed specimen has the shape of a bending plate. Optimization of the load input situation for getting low stress gradients as possible have been performed by finite element method. The three dimensional stress analyses were carried out by isoparametric volume elements with 20 nodes with the FE program ADINA on a machine of type CYBER-175. Because of symmetry it was sufficient to regard only one quarter of the shape and one half of thickness of the specimen. Results are shown in Fig. 3 for instance on a plate of 400 mm square and 60 mm thickness without a crack. The nominal stresses σ_{yy} and σ_{zz} in z-direction (parallel to the crack front) have a common maximum in the center of the plate. While σ_{yy} and σ_{zz} have pronounced gradients in z-direction under "five point" loading the stress gradients will be lowered by changing from "five point" to "eight point loading" as demonstrated in the lower part of the figure. In addition there is a range in the center of the plate where within the dimension of the initial crack the gradients of both stresses are about zero. This means a sufficient homogeneous stress distribution is expected to be applied in the neighborhood of the initial crack. The ratio of the nominal stresses σ_{yy}/σ_{zz} may be influenced within wide limits by changing the ratio of length to width of the plate.

3. Material and experimental details

The tests were carried out on the German Standard Steel StE 47 which is a micro alloyed weldable fine grained normalized structural steel. The chemical composition and the mechanical properties of the steel are represented in Table 1.

For the comparison of the influence of stress state on the test results two types of specimens were used. Both types of specimens were produced from hot-rolled plates of 60 mm thickness. The first type of specimen on which the influence of the biaxial stress state should be examined is shown in Fig. 4. The square plate is provided with a semi-elliptical crack which is produced by machining to a depth of 15 mm and by bending fatigue up to a maximum depth of 23 mm. The direction of crack extension is perpendicular to the rolling direction. The specimen is subjected to "eight point" bending by rollers of 80 mm diameter in the corners on one side of the plate and by four loading spheres of the same diameter which have a diagonal distance of 120 mm, on the other side of the plate. A nominal stress distribution similar to that shown in the lower part of Fig. 3 is expected at the crack front. The second type of specimen is a usual single-edge-crack three point bending specimen of 80 mm width and 210 mm length as shown in Fig. 5. The initial crack is provided in the same manner as for the plate shaped specimen. The loading rollers have a diameter of 60 mm.

Before tests were performed on the plate shaped specimens strain gage measurements around the crack were carried out to ensure that symmetric loading takes place and the desired nominal stress ratio $\sigma_{yy}/\sigma_{zz} = 1$ is achieved. The tests were carried out in the temperature range 0 to -100° C including the temperature at which general yield is expected. The specimen temperature is measured by thermocouples attached at the rear of the crack. The crack opening displacement is measured by clip gages. The same test procedure is used in the tests on the three point bending specimens.

4. Results

To compare the test results of both types of specimens in terms of fracture toughness values K_{Ic} or J_{Ic} the calculation of the stress intensity factors according the individual specimen shape is necessary. For the plate shaped specimen this can be done only by finite element method under the elastic-plastic regime. Preparations for such calculations are already running but as the time being the influence of stress state on fracture toughness can be concluded only by comparison of figures directly got from tests on both types of specimens, such as fracture force F_f, plástic crack opening displacement (COD) δ_f and depth of stable crack a_s as functions of test temperature. Such results are shown in Fig. 6 for the plate shaped specimen. In the upper diagram the fracture force F_f normalized on the force for general yield F_{gy} is plotted as a function of temperature. At the value $F_f/F_{gy} = 1$ the temperature for general yield T_{gy} is -16^o C for the plate shaped specimen. At this temperature the plastic crack opening displacement δ_f has just reached the value $\delta_{gy} = 0.25$ mm as the diagram in the middle of Fig. 6 demonstrates. In the lower diagram of Fig. 6 where the depth of stable crack growth a_s is plotted in dependence on temperature, the temperature T_s at which stable crack growth starts, is marked. $T_s = -10^o$ C indicates that there is only a small difference between the temperature T_{gy} for general yield and the temperature T_s for the start of stable crack growth. Fig. 7 represents the results of the tests on the three point bending specimens. The temperature for general yield T_{gy} is here about -50^o C and the temperature for the start of stable crack growth T_s has a value of about -40^o C; again the difference of both temperatures is relatively small. The results for both types of specimens were compared in Fig. 8. A first view already indicates that the curves will be shifted to higher temperatures if the type of specimen is changed from the three point specimen (I) to the plate shaped specimen (II). So the temperature for general yield is increased by $\Delta T_{gy} = 34$ K and the temperature for the start of stable crack growth by $\Delta T_s = 30$ K. Thus these direct results of tests without any further detailed analysis give already a strong support that biaxial loading by an additionally imposed stress σ^e_{zz} parallel to the crack front will shift the temperature for general yield to a higher temperature compared with simple plane strain conditions and therefore will decrease the fracture toughness; both effects are caused by enhancement of the multiaxiality of stress state.

Further tests on bigger specimens are in preparation and the three dimensional stress analysis ahead the crack front as well in the elastic as in the elastic-plastic range by FEM will help for further clarification and evaluation of this important phenomenon in the near future.

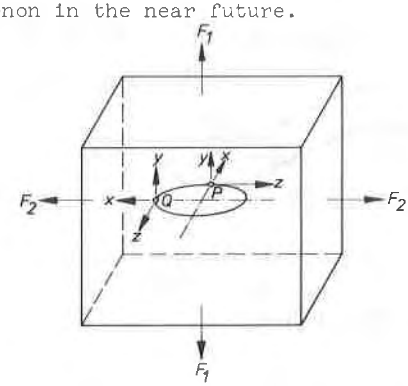

Fig. 1 Coordinate system at a penny shaped crack in a biaxial stressed structural member

References

[1] Liebowitz, H., J. Eftis and D.L. Jones: Fracture 1977, Vol. 1, ICF4, Waterloo, Canada, 695-724
[2] Liebowitz, H. and J. Eftis: 4th SMiRT-Conf., Vol. G, Paper G 5/1
[3] Aurich, D.: Fract. Mech., 7 (1975), 761-765
[4] Aurich, D., R. Helms, P. Schmidt, H. Veith and J. Ziebs: 4th SMiRT-Conf., Vol. G, Paper G 5/1
[5] Griffiths, J.R. and D.R.J. Owen: J. Mech. Phys. Sol. 19 (1971), 419-431
[6] Ewing, D.J. and J.R. Griffiths: J. Mech. Phys. Sol. 19 (1971), 389-394
[7] Kochendörfer, A.: Z. Metallkde. 62 (1971), 1-12
[8] Knott, J.F.: Fundamentals of Fracture Mechanics, London, Butterworths 1975
[9] Tetelman, A.S., T.R. Wilshaw and C.A. Ran: Int. J. Fract. Mech. 4 (1968), 142-157 and Eng. Fract. Mech. 1 (1968), 191-211

Table 1: Chemical composition and mechanical properties

Chemical composition, wt %

C	Si	Mn	P	S	Al	Co	Cr
0.155	0.38	1.79	0.019	<0.004	0.045	<0.005	0.011

Cu	Mo	Nb	Ni	Ta	Ti	V	[illegible]
0.015	<0.005	0.002	0.33	<0.010	<0.003	0.178	0.005

Mechanical Properties

Tensile Strength N/mm^2	Yield Strength N/mm^2	Elongation in 5 D_o %	ISO-V-notch toughness at -20°C longitudinal J	long transverse J
634	512	26	104	111

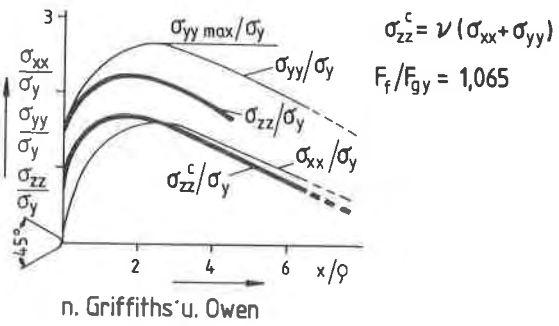

Fig. 2 Stresses in the plastic zone ahead 45°-notch

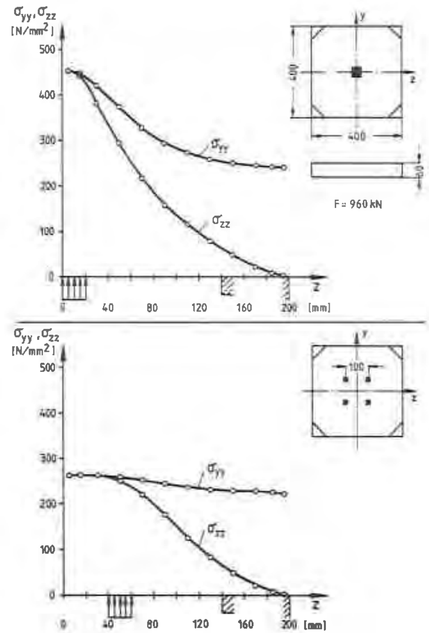

Fig. 3 Influence of loading conditions on the stress distribution in a quadratic plate

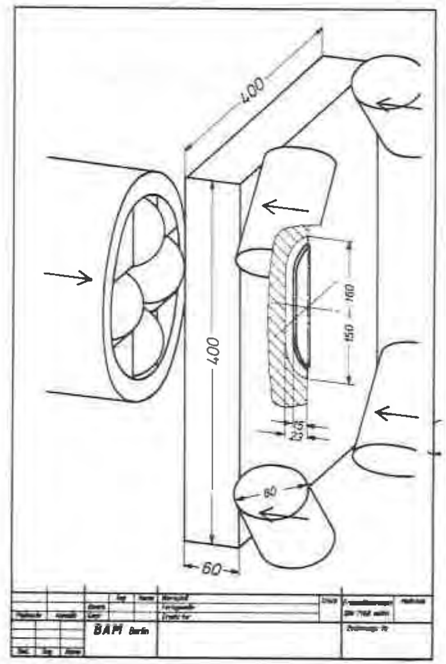

Fig. 4 Dimensions of the plate shaped specimen and loading conditions

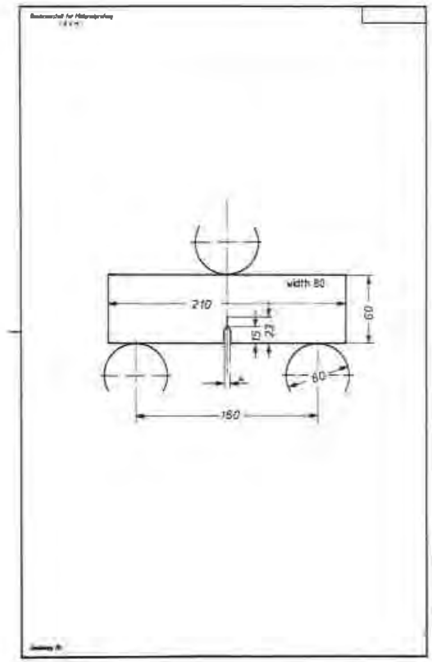

Fig. 5 Dimensions of the three point bending specimen and loading conditions

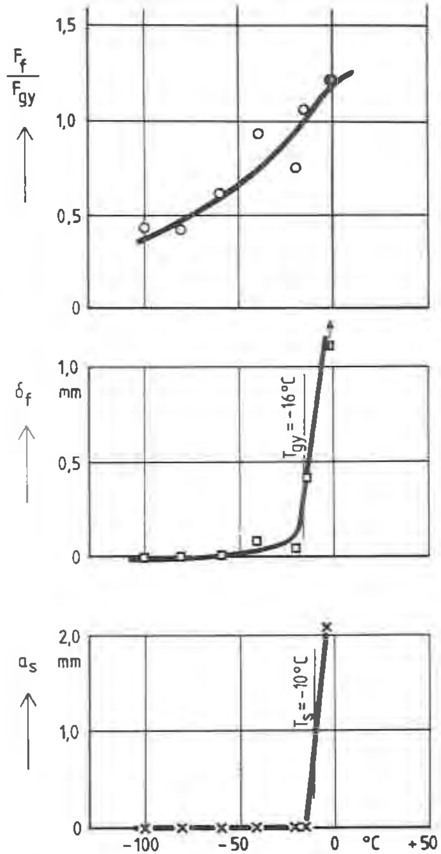

Fig. 6 Fracture load F_f normalized on the load for general yield F_{gy}, plastic COD δ_f and depth of stable crack growth a_s as functions of test temperature for the plate shaped specimen

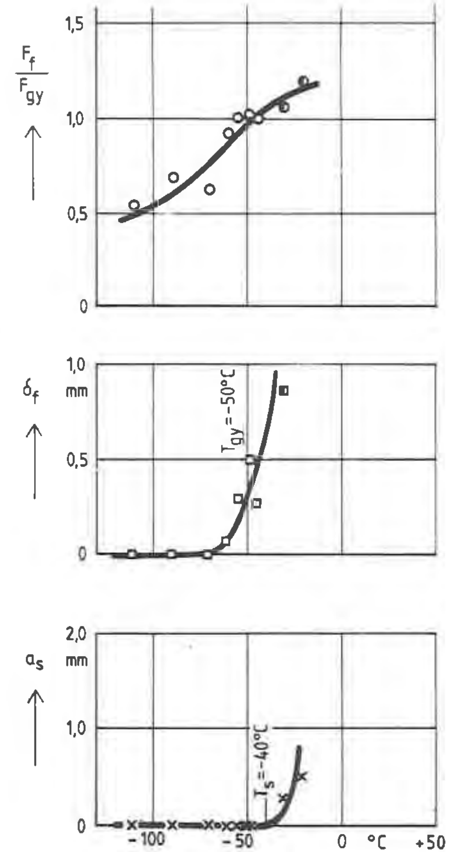

Fig. 7 Fracture load F_f normalized on the load for general yield F_{gy}, plastic COD δ_f and depth of stable crack a_s as functions of test temperature for the three point bending specimen

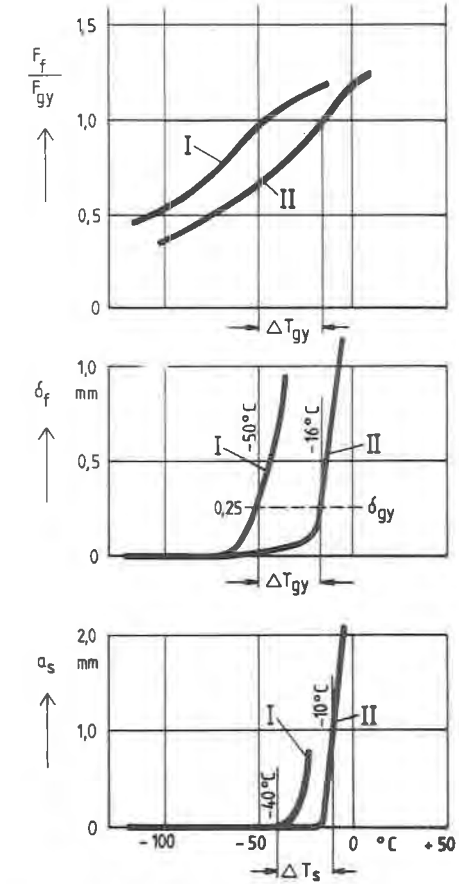

Fig. 8 Comparison of fracture load F_f normalized on the load for generally yield F_{gy}, the plastic COD δ_f and depth of stable crack a_s for the three point bending specimen (I) and the plate shaped specimen (II).